BNL-108442-2015-JA

Accepted Manuscript

Characterization of Cu(In,Ga)Se_2 (CIGS) films with varying gallium ratios

Jesse Claypoole, Bernadette Peace, Neville Sun, Dan Dwyer, Matthew D. Eisaman, Pradeep Haldar, Harry Efstathiadis

PII: S0925-8388(15)30982-8

DOI: 10.1016/j.jallcom.2015.09.006

Reference: JALCOM 35281

To appear in: *Journal of Alloys and Compounds*

Received Date: 14 May 2015

Revised Date: 30 August 2015

Accepted Date: 1 September 2015

Please cite this article as: J. Claypoole, B. Peace, N. Sun, D. Dwyer, M.D. Eisaman, P. Haldar, H. Efstathiadis, Characterization of Cu(In,Ga)Se_2 (CIGS) films with varying gallium ratios, *Journal of Alloys and Compounds* (2015), doi: 10.1016/j.jallcom.2015.09.006.

This is a PDF file of an unedited manuscript that has been accepted for publication. As a service to our customers we are providing this early version of the manuscript. The manuscript will undergo copyediting, typesetting, and review of the resulting proof before it is published in its final form. Please note that during the production process errors may be discovered which could affect the content, and all legal disclaimers that apply to the journal pertain.

ACCEPTED MANUSCRIPT

Characterization of $Cu(In,Ga)Se_2$ (CIGS) films with varying gallium ratios

Jesse Claypoole[1], Bernadette Peace[1], Neville Sun[2], Dan Dwyer[1], Matthew D. Eisaman[3], Pradeep Haldar[1] and Harry Efstathiadis[1]

[1]State University of New York Polytechnic Institute, Colleges of Nanoscale Science and Engineering, 257 Fuller Rd., Albany, NY 12203, USA

[2]Angstrom Sun Technologies Inc., 31 Nagog Park, Acton, MA 01720, USA

[3] Sustainable Energy Technologies Department, Brookhaven National Laboratory, Upton , NY 11973, USA. Department of Physics and Astronomy, Stony Brook University, Stony Brook, NY 11794, USA. Department of Electrical and Computer Engineering, Stony Brook University, Stony Brook, NY 11794, USA.

Abstract

$Cu(In_{1-x},Ga_x)Se_2$ (CIGS) absorber layers were deposited on molybdenum (Mo) coated soda-lime glass substrates with varying Ga content (described as Ga/(In+Ga) ratios) with respect to depth. As the responsible mechanisms for the limitation of the performance of the CIGS solar cells with high Ga contents are not well understood, the goal of this work was to investigate different properties of CIGS absorber films with Ga/(In+Ga) ratios varied between 0.29 and 0.41 (as determined by X-ray florescence spectroscopy (XRF)) in order to better understand the role that the Ga content has on film quality. The Ga grading in the CIGS layer has the effect causing a higher bandgap toward the surface and Mo contact while the band gap in the middle of the CIGS layer is lower. Also, a wider and larger Ga/(In+Ga) grading dip located deeper in the CIGS absorber layers tend to produce larger grains in the regions of the films that have lower

ACCEPTED MANUSCRIPT

Ga/(In+Ga) ratios. Moreover, it was found that surface roughness decreases from 51.2 nm to 41.0 nm with increasing Ga/(In+Ga) ratios. However, the surface roughness generally decreases if the Ga grading occurs deeper in the absorber layer.

Keywords: Energy Storage Materials, Semiconductors, Thin Films, Photovoltaics, Atomic Force Microscopy (AFM), Scanning Electron Microscopy (SEM)

Corresponding Author:
Email: JClaypoole@sunypoly.edu
Tel: 804-523-0756
Postal: State University of New York Polytechnic Institute,
Colleges of Nanoscale Science and Engineering
257 Fuller Road
Albany, NY 12203

ACCEPTED MANUSCRIPT

ACCEPTED MANUSCRIPT

1. Introduction

$Cu(In_{1-x},Ga_x)Se_2$ (CIGS) films currently holds the record for thin-film photovoltaic (PV) power-conversion efficiency at 21.7 %, and are approaching the efficiency of conventional silicon solar cells [1]. Two of the reasons that CIGS thin-film devices are being developed, is that they have a direct band gap and are less expensive to fabricate than PV devices made of silicon [2]. Some of the key features of the CIGS-based compounds are that the material system has a tunable band gap (from 1.0 - 1.7 eV) and lattice parameters that can be adjusted by changing the Ga content in the absorber layer. It has also been shown that increased Ga/(In+Ga) leads to smaller grain sizes [3].

The optimal efficiency of CIGS devices should occur at the band gap of ~1.5 eV, which corresponds to a Ga fraction (x = Ga/(In+Ga)) ~0.6 - 0.7) . However, in high-performance CIGS solar cells, the CIGS films typically have a Ga ratio of around x = 0.3, corresponding to a band gap energy of approximately 1.15 eV. For Ga ratios that exceed 0.3, the overall performance of the CIGS solar cells begins to diminish [4].

In this work, the properties of CIGS absorber films deposited by a 3-stage co-evaporation process with Ga/(In+Ga) ratios varied between 0.29 and 0.41 are investigated. The goal of this study is to correlate Ga/(In+Ga) ratios with film properties in order to better understand the role that the Ga content has on film quality.

2. Material and Methods

The polycrystalline CIGS absorber layer of the cells was deposited at a thickness of 2 μm on soda-lime glass which had been coated with a 1 mm Mo layer. The deposition procedure of the CIGS absorber layer was a 3-stage thermal co-evaporation of the individual elemental components which was done at the US PVMC facility in Halfmoon, NY described elsewhere [5].

CIGS samples were prepared with x ranging from 0.29 to 0.41, as determined by X-ray florescence spectroscopy (XRF). Film composition was measured using a SII Nanotechnology SEA2210A X-ray florescence spectrometer (XRF). The XRF was calibrated using inductively coupled plasma mass spectrometry (ICP). All reported values were measured at the center of the 10 cm x 10 cm substrate. To investigate the effects of Ga/(In+Ga) ratio, Ga and In fluxes were regulated by the temperature of effusion cells in the first stage, while the Cu/(In+Ga) ratio was kept at 0.80 - 0.90 for all the samples.

Secondary ion mass spectroscopy (SIMS) depth profiles on devices grown using this process were used to obtain composition profiles of the CIGS. The MS (Mass Spectroscopy) SIMS characterization of the CIGS sample was carried out on the Physical Electrons 6650 Quadrupole SIMS. The samples were first loaded into the sample exchange chamber and pumped down to 10^{-8} torr before being inserted to the main chamber. Cesium bombardment with a 60 degree angle of incidence, an accelerating voltage of 5 keV, and a beam current of 450 nA was used at 10^{-9} torr in order to create the ions. The area scanned by the cesium beam had a raster size of 500 x 500 µm and a 10% gate detection area. An electron multiplier detector was used to detect the positive secondary ions. Depth calibration was made based on profilometry of sputter crater depth in CIGS. Concentration calibration was made by measuring a CIGS reference of comparable composition, which has a known composition determined by Rutherford backscattering.

The morphology of the CIGS layers were examined by scanning electron microscopy (SEM) using a Zeiss1550. Atomic force microscopy (AFM) characterization was performed using a Nanosurf FlexAFM research tool operating in tapping mode. The height and phase images were measured using an ACLA silicon cantilever probe made by Applied

NanoStructures, Inc., with a tip radius of ~10 nm, a frequency range of 160-225 kHz, and an average spring constant (k) of 58 N/m.

The CIGS film thickness and optical constants n and k were obtained by using a spectroscopic ellipsometer TFProbe SE500BA, developed by Angstrom Sun Technologies Inc. The spectroscopic ellipsometry technique measures the physical and optical properties on any section of the film without direct physical contact with the film surface. The TFProbe SE500BA detector covers a wavelength range from 250 nm to 1700 nm and is equipped with an advanced automatic variable incident angle precision goniometer. The CIGS samples were measured at 67.5, 70, and 72.5 degree incident angles with 512 wavelength points.

The relative change in phase and amplitude information is acquired by the ellipsometer and translated into Psi (Ψ) and Delta (Δ) parameters. A theoretically calculated set of modeled parameters is fitted with the ellipsometer measured parameters to acquire the thickness and optical property of the CIGS films. The parameter Ψ is defined by equation 1.

$$\rho = \frac{R^P}{R^S} = Tan\Psi \cdot \mathrm{e}^{j\Delta} \qquad (1)$$

Equation 1 includes the complex Fresnel reflection coefficients R^P and R^S representing the reflected parallel component (P) and the perpendicular component (S) relative to the incident plane, respectively. Parameter Δ is the phase difference induced by the reflection and it is obtained by analyzing the film stack and substrate in the system.

A Tauc-Lorentz dispersion model, calculated by the TFProbe 3.3 software, was applied on the measured data sets to obtain the optical properties of the CIGS films [6]. The imaginary

part of the dielectric function ε_i was developed by Jessison and Modine in 1996 [7], by multiplying the Tauc joint density of states with the Lorentz oscillator:

$$\varepsilon_i(E) = \frac{AE_0C(E-E_G)^2}{((E^2-E_0)^2+C^2E^2)E}, \quad E > E_g, \tag{2}$$

$$\varepsilon_i(E) = 0, \quad E \leq E_g, \tag{3}$$

where E_0 is the peak transition energy, C is the broadening term, E_g is the optical band gap, and A is proportional to the transition probability matrix element [8].

The real part of the dielectric function ε_r is calculated by Kramers-Kronig integration:

$$\varepsilon_r(E) = E_{inf} + \frac{2P}{\pi}\int_{E_g}^{\infty} \frac{\xi\,\varepsilon_i(\xi)}{\xi^2 - E^2} d\xi, \tag{4}$$

The fitting parameters in the software utilizes the variables A, C, E_0, E_g and E_{inf} from the Tauc-Lorentz model.

When studying optical property over a very wide wavelength range, especially for photovoltaic films, the Tauc-Lorentz dispersion is inadequate to describe the dielectric response completely. Therefore, five Lorentz type oscillators were added into the total dielectric function in the analysis [9]:

$$\varepsilon_r = \frac{A_1\lambda^2(\lambda^2-L_0{}^2)}{(\lambda^2-L_0{}^2)^2+\gamma^2\lambda^2} \tag{5}$$

$$\varepsilon_i = \frac{A_1\lambda^3\gamma}{(\lambda^2-L_0{}^2)^2+\gamma^2\lambda^2} \tag{6}$$

ACCEPTED MANUSCRIPT

where λ is the wavelength, A_1 is the amplitude, L_0 is the central wavelength, and γ is the width of the oscillators. These three variable parameters are then fitted during regression.

The Levenberg-Marquardt algorithm (LMA), a non-linear least-squares method, is used for modeling. The best fitted variables can be found by minimizing χ^2:

$$\chi^2 = \frac{1}{2n-m-1}\sum_{i=1}^{n}\left[\left(Tan\Psi_{Theory}^{i} - Tan\Psi_{Exp}^{i}\right)^2 + \left(Cos\Delta_{Theory}^{i} - Cos\Delta_{Exp}^{i}\right)^2\right] \quad (7)$$

where $Tan\Psi_{Theory}$ and $Cos\Delta_{Theory}$ are the modeled values, $Tan\Psi_{Exp}$ and $Cos\Delta_{Exp}$ are measured values, m is the number of variables to be fitted, and n is the number of data points [10]. The fitting process seeks to adjust those variables that could minimize the value χ^2. It is clear that more data points and fewer variables would make fitting results more reliable and with smaller uncertainty. Therefore, variable incident angle data sets will produce higher quality ellipsometry analysis results in general.

3. Results & Discussion

The CIGS films characterized in this study were deposited with Ga/(In+Ga) ratios (x) ranging from 0.29 to 0.41 as determined by x-ray florescence spectroscopy (XRF). Ga/(In+Ga) ratios are listed in Table 1. Moreover, secondary ion mass spectroscopy (SIMS) was the analytical technique employed to obtain quantitative depth profiles for each sample. Figures 1-4 display the SIMS depth profiles of Cu, In, Ga, Se and Na concentrations (in atomic %) as a function of depth for each sample. Figure 5 depicts the combined SIMS depth profiles of the Ga/(In+Ga) ratio for all CIGS samples and it allows for a comparison of how the Ga ratio varies through the depth of each film. It can be seen in Figure 5 that all CIGS samples have a Ga/(In+Ga) grading dip, which is related to the 3-stage deposition process. Furthermore, it can

be seen in Figure 5 that this Ga/(In+Ga) grading dip occurs in a region near the center of the depth of the absorber layer for all samples. The SIMS results presented in Figure 5 were used in conjunction with ellipsometry to calculate the band gap for these samples assuming the films were inhomogeneous. That is, the ellipsometry model was built assuming the CIGS layer was separated into three (3) regions (indicated as Region 1 through Region 3). These ellipsometry results are presented in Tables 2-4. The depths used in the regions are shown in Table 5. For each CIGS sample, it was assumed that Region 1 and Region 3 were equivalent in order to simplify the model, as the Ga/(Ga+In) values were very close. The index profiles of Region 2 were thus modeled differently while the index profiles for Region 1 and Region 3 were kept the same as each other.

By observing Tables 2-4, it can be seen that the band gaps for all CIGS samples in Region 1 and Region 3 are always higher than Region 2. This corresponds to the Ga grading dip present in all CIGS samples, as demonstrated in Figure 5. Moreover, it can be observed in Table 3 that the ellipsometry band gap results trend with the average Ga/(In+Ga) ratios as measured by XRF for each sample. The band gap values increase proportionally with the Ga/(In+Ga) ratio, which has been reported previously by other groups [11,12]. This trend is also present in Region 1 and Region 3. It was observed that sample C has a slightly higher band gap than sample D even though sample C has a lower Ga/(In+Ga) ratio than sample D as determined by XRF and shown in Table 2 and Table 4.

Additionally, utilizing SIMS combined with scanning electron microscopy (SEM) characterization techniques, it has been confirmed that as Ga content (x = Ga/(In+Ga)) increases, the grain size of the CIGS decreases, which has been also been reported by other groups [3,12]. The data displayed in Figure 5 can also be compared with the SEM cross-sectional images

ACCEPTED MANUSCRIPT

presented in Figure 6 in order to explain the variations in grain sizes throughout the depth of the films for each sample. Since the Ga/(In+Ga) grading dip occurs in a region near the center of the depth of the absorber layer for all samples, one would expect the largest grain sizes to be located in this area. This expectation can be confirmed by comparing the Ga ratio depth profiles in Figure 5 with the corresponding SEM cross-sectional images in Figure 6. Sample A has intermediate average grain sizes (columnar-shaped grains approximately 1 µm in height) compared to samples B and C due to the broad dip in the Ga/(In+Ga) ratio and higher average Ga/(In+Ga) ratio of sample A. The smallest grains in sample A are found near the surface and the Mo interface. This corresponds to where the Ga/(In+Ga) ratio is the highest, as can be seen in Figure 5. Sample B has a greater number of larger grains (at about 0.75 - 1µm) throughout the depth of the film compared to the other samples. This is due to sample B's very broad Ga/(In+Ga) grading at relativity low average Ga/(In+Ga) ratios. Sample C's lowest Ga/(In+Ga) ratio at the lowest portion of this sample's Ga/(In+Ga) grading is almost the same as that in B. Sample C does not have average grain sizes (approximately 0.5 um) as large as sample B, though sample C has larger grains that are located closer to the surface than sample B. In contrast to sample C, sample B has larger grains located deeper in the absorption layer (closer to the back Mo layer).

By comparing Figure 5 and Figure 6, it is clear that sample D has the smallest average grain sizes (only about 200 nm) due to this sample containing the highest average Ga/(In+Ga) ratio and steepest Ga/(In+Ga) grading. Moreover, as with samples A through sample C, the largest grains in sample D are located where the Ga/(In+Ga) ratio is the lowest..

The surface roughness of CIGS samples A through D were determined by atomic force microscopy (AFM), and are listed in Table 6. The roughness values of each sample cannot be

ACCEPTED MANUSCRIPT

explained by solely investigating the Ga/(In+Ga) ratios since the position of the Ga/(In+Ga) grading dip (as defined by SIMS depicted in Figure 5) determines the position of the larger grains in the absorber layer. Sample D has the largest average Ga/(In+Ga) ratio, and thus the smallest grains and lowest surface roughness (41.0 nm), as expected. Sample A has the second highest Ga/(In+Ga) ratio at the top surface, and thus a slightly lower surface roughness (45.7 nm). It is interesting to note that while sample C has a higher surface roughness (51.2 nm) than sample B (47.5 nm), sample C has a higher Ga/(In+Ga) ratio. This can be explained by how the Ga/(In+Ga) grading dip in sample C is shifted towards the top surface, which results in larger grains formed closer to the surface, as illustrated in Figure 6. In contrast, Figure 6 shows sample B to have a greater number of larger grains, though the grading dip occurs deeper in the absorber layer so smaller grains are positioned on top of the larger grains. This accounts for the decreased surface roughness in sample B. The reason the position of the Ga dip is important is because the surface roughness can affect the interface between the n type layer and the CIGS.

4. Conclusions

The Ga/(In+Ga) ratio and depth of the Ga/(In+Ga) grading dip effects the band gap, grain structure, and surface roughness of the CIGS samples studied. The band gaps for all CIGS samples in the regions defined towards the top surface and back Mo contact are always higher (Regions 1 and 3) than towards the center of the depth of the film (region 2). This corresponds to the Ga grading dip present in all CIGS samples. Wider Ga/(In+Ga) grading dips located deeper in the absorber layers tend to produce larger grains in the regions of the absorber layer that have lower Ga/(In+Ga) ratios. Moreover, it was found that surface roughness decreases with increasing Ga/(In+Ga) ratios. Though, this surface roughness decreases if the Ga grading occurs deeper in the absorber layer rather than towards the top surface of the samples.

ACCEPTED MANUSCRIPT

ACCEPTED MANUSCRIPT

Acknowledgments
This work was supported by the United States Department of Energy (DOE) award number: DE-EE0004947. This work was partially supported by the U.S. Department of Energy, Sustainable Energy Technologies Department under Contract No. DE-SC0012704, and Brookhaven National Laboratory's Laboratory Directed Research and Development (LDRD) Program.

References

[1] P. Jackson, D. Hariskos, R. Wuerz, O, Kiowski, A. Bauer, T. M. Friedlmeier, Phys. Status Solidi-RRL 9, No. 1, 28-31 (2015)

[2] Green, Martin A., et al. "Solar cell efficiency tables (version 46). *Progress in Photovoltaics: Research and Applications* 23.7 (2015): 805-812

[3] T. Higuchi, N. Usami, T. Minemoto, Phys. Status Solidi C 10, No. 7-8, 1035-1037 (2013)

[4] Huang, Chia-Hua, Journal of Physics and Chemistry of Solids 69, 330–334 (2008)

[5] D. Dwyer, S. Schujman, J. Novak, D. Metacarpa, P. Haldar, "Selenium flux effects on $Cu(In,Ga)Se_2$ growth rate, and control by in-line X-ray fluorescence" Proc. of the 39rd IEEE Photovoltaic Specialists Conference, June 16-21, 2013, Tampa, FL, pp. 1957-1960

[6] TFProbe 3.3 Anstrom Sun technologies INC, Acton MA, 2009, software available at http://www.angstec.com/

[7] G. E. Jellison and F.A. Modine, Appl Phys Lett. 69, 371-374 (1996)

[8] Tompkins, H. G., & Irene, G. E. Jellison, E. A. (2005). Handbook of Ellipsometry. Norwich, NY: William Andrew, Inc. Ch 3, 256-258

[9] Hummel, R. (1993). *Electronics Properties of Materials* (Second ed.). New York: Springer-Verlag Berlin Heidelberg

ACCEPTED MANUSCRIPT

[10] Press, W., Teukolsky, S., Vetterling, W., & Flannery, B. (1992). *Numerical Recipes in C: The Art of Scientific Computing* (Second ed.). Cambridge: Press Syndicate of the University of Cambridge

[11] G. Hanna, A. Jasenek, U. Rau, and H.W. Schock, Thin Solid Films, 387, 71-73 (2001)

[12] Sunghun Junga, SeJin Ahna, Jae Ho Yuna, Jihye Gwaka, Donghwan Kimb, and Kyunghoon Yoona, Current Applied Physics 10 990-996 (2010)

ACCEPTED MANUSCRIPT

ACCEPTED MANUSCRIPT

List of Tables and Figures

Table 1: CIGS sample identifications with corresponding depth averaged Ga/(In+Ga) ratios as determined by XRF.

Table 2: CIGS Region 1 band gap estimations as determined by ellipsometry with corresponding sample average Ga/(In+Ga) ratio as determined by XRF.

Table 3: CIGS Region 2 band gap estimations as determined by ellipsometry with corresponding sample average Ga/(In+Ga) ratio as determined by XRF.

Table 4: CIGS Region 3 band gap estimations as determined by ellipsometry with corresponding sample average Ga/(In+Ga) ratio as determined by XRF.

Table 5: Depth range used in ellipsometry calculations to calculate bandgaps in regions 1, 2, and 3

Table 6: Surface roughness as determined by atomic force microscopy (AFM) for each CIGS sample.

Figure 1: Secondary ion mass spectroscopy (SIMS) quantitative depth profile for sample A presenting Cu (blue), In (red), Ga (yellow), Se (purple), and Na (green) elemental concentrations (in atomic %) as a function of depth (nm). Exact values for the regions 1-3 are shown in Table 5.

Figure 2: Secondary ion mass spectroscopy (SIMS) quantitative depth profile for sample B presenting Cu (blue), In (red), Ga (yellow), Se (purple), and Na (green) elemental concentrations (in atomic %) as a function of depth (nm). Exact values for the regions 1-3 are shown in Table 5.

Figure 3: Secondary ion mass spectroscopy (SIMS) quantitative depth profile for sample C presenting Cu (blue), In (red), Ga (yellow), Se (purple), and Na (green) elemental concentrations (in atomic %) as a function of depth (nm). Exact values for the regions 1-3 are shown in Table 5.

ACCEPTED MANUSCRIPT

ACCEPTED MANUSCRIPT

Figure 4: Secondary ion mass spectroscopy (SIMS) quantitative depth profile for sample D presenting Cu (blue), In (red), Ga (yellow), Se (purple), and Na (green) elemental concentrations (in atomic %) as a function of depth (nm). Exact values for the regions 1-3 are shown in Table 5.

Figure 5: Combined secondary ion mass spectroscopy (SIMS) quantitative depth profiles displaying the Ga/(In+Ga) ratio for each sample: A (blue), B (red), C (green) and D (purple) as a function of depth (nm).

Figure 6: Scanning electron microscopy (SEM) cross sectional images of sample A (top left), sample B (top right), sample C (bottom left), and sample D (bottom right).

ACCEPTED MANUSCRIPT

ACCEPTED MANUSCRIPT

Sample	Ga/(In+Ga)
A	0.29
B	0.32
C	0.35
D	0.41

Table 1. CIGS sample identifications with corresponding Ga/(In+Ga) ratios as determined by XRF

ACCEPTED MANUSCRIPT

ACCEPTED MANUSCRIPT

Sample	Ga/(In+Ga)	Thickness (nm)	±Uncertainty (nm)	Eg (eV)	±Uncertainty (eV)
A	0.29	368.4	5.733	1.169	0.0752
B	0.32	389.9	5.448	1.188	0.1107
C	0.35	321.1	5.625	1.443	0.0977
D	0.41	254.8	4.474	1.437	0.0978

Table 2. CIGS Region 1 band gap estimations as determined by ellipsometry with corresponding sample average Ga/(In+Ga) ratio as determined by XRF

ACCEPTED MANUSCRIPT

ACCEPTED MANUSCRIPT

Sample	Ga/(In+Ga)	Thickness (nm)	±Uncertainty (nm)	Eg (eV)	±Uncertainty (eV)
A	0.29	900.2	11.72	1.055	0.04030
B	0.32	932.6	7.210	1.075	0.1002
C	0.35	873.4	6.006	1.075	0.0490
D	0.41	936.3	6.837	1.141	0.4705

Table 3. CIGS Region 2 band gap estimations as determined by ellipsometry with corresponding sample average Ga/(In+Ga) ratio as determined by XRF

ACCEPTED MANUSCRIPT

ACCEPTED MANUSCRIPT

Sample	Ga/(In+Ga)	Thickness (nm)	±Uncertainty (nm)	Eg (eV)	±Uncertainty (eV)
A	0.29	1608	10.91	1.169	0.07520
B	0.32	1665	11.19	1.188	0.1107
C	0.35	1791	13.31	1.443	0.0977
D	0.41	1829	8.495	1.437	0.0978

Table 4. CIGS Region 3 band gap estimations as determined by ellipsometry with corresponding sample average Ga/(In+Ga) ratio as determined by XRF

ACCEPTED MANUSCRIPT

ACCEPTED MANUSCRIPT

	Region 1 (depth nm)	Region 2 (Depth nm)	Region 3 (Depth nm)
Sample A	0 – 368	368 – 1268	1268.66 – 2876
Sample B	0 – 389	389 – 1322	1322.49 – 2897
Sample C	0 – 321	321 – 1194	1194.55 – 2985
Sample D	0 – 354	354 – 1290	1290.64 – 3119

Table 5. Depths range used in ellipsometry calculations to calculate bandgaps in regions 1, 2, and 3

ACCEPTED MANUSCRIPT

ACCEPTED MANUSCRIPT

Sample	Roughness (nm)
A	45.7
B	47.5
C	51.2
D	41.0

Table 6. Surface roughness as determined by atomic force microscopy (AFM) for each CIGS sample

ACCEPTED MANUSCRIPT

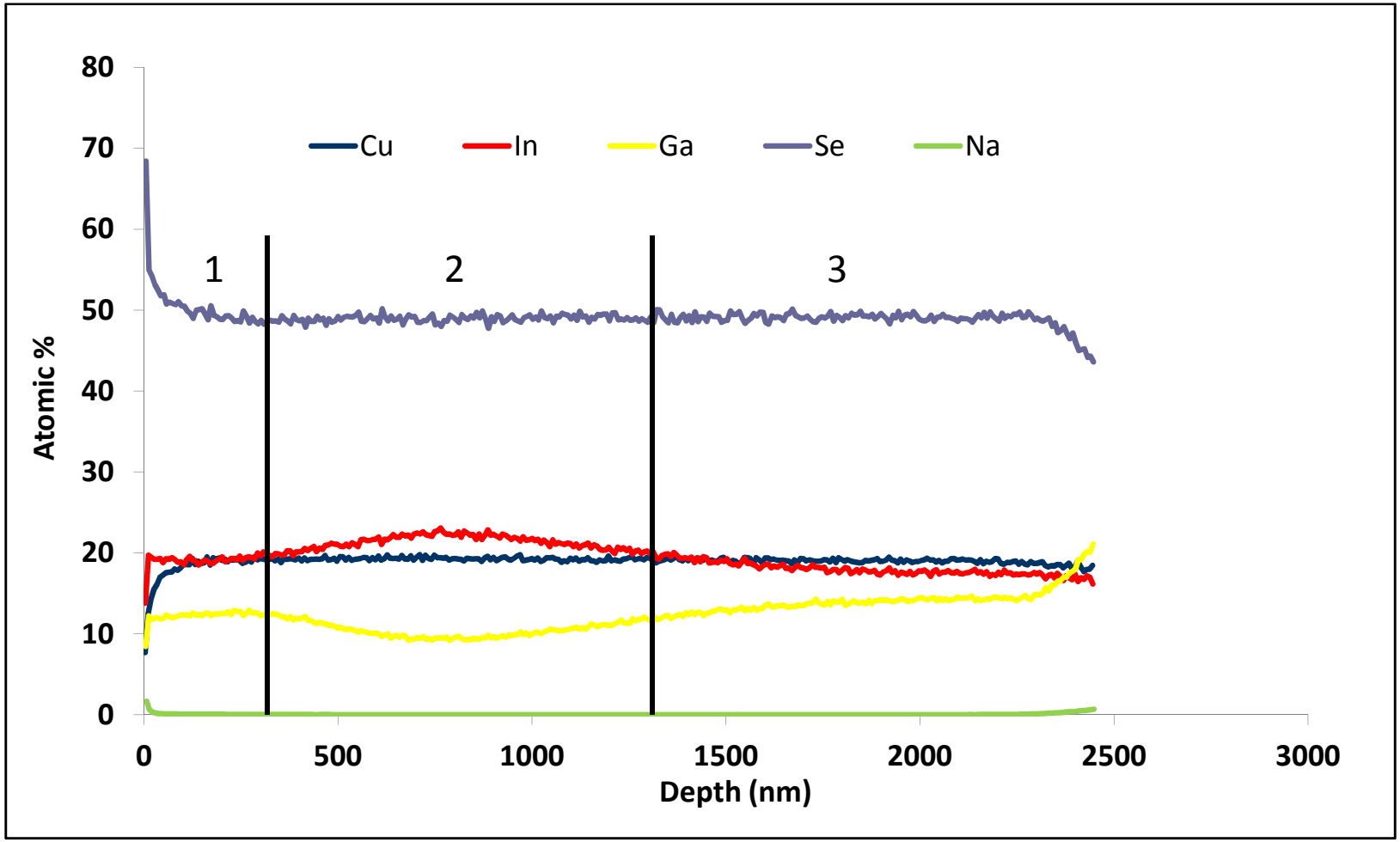
80
70
60
50
40
30
20
10
0
Atomic %
Cu
In
Ga
Se
Na
1
2
3
0
500
1000
1500
2000
2500
3000
Depth (nm)

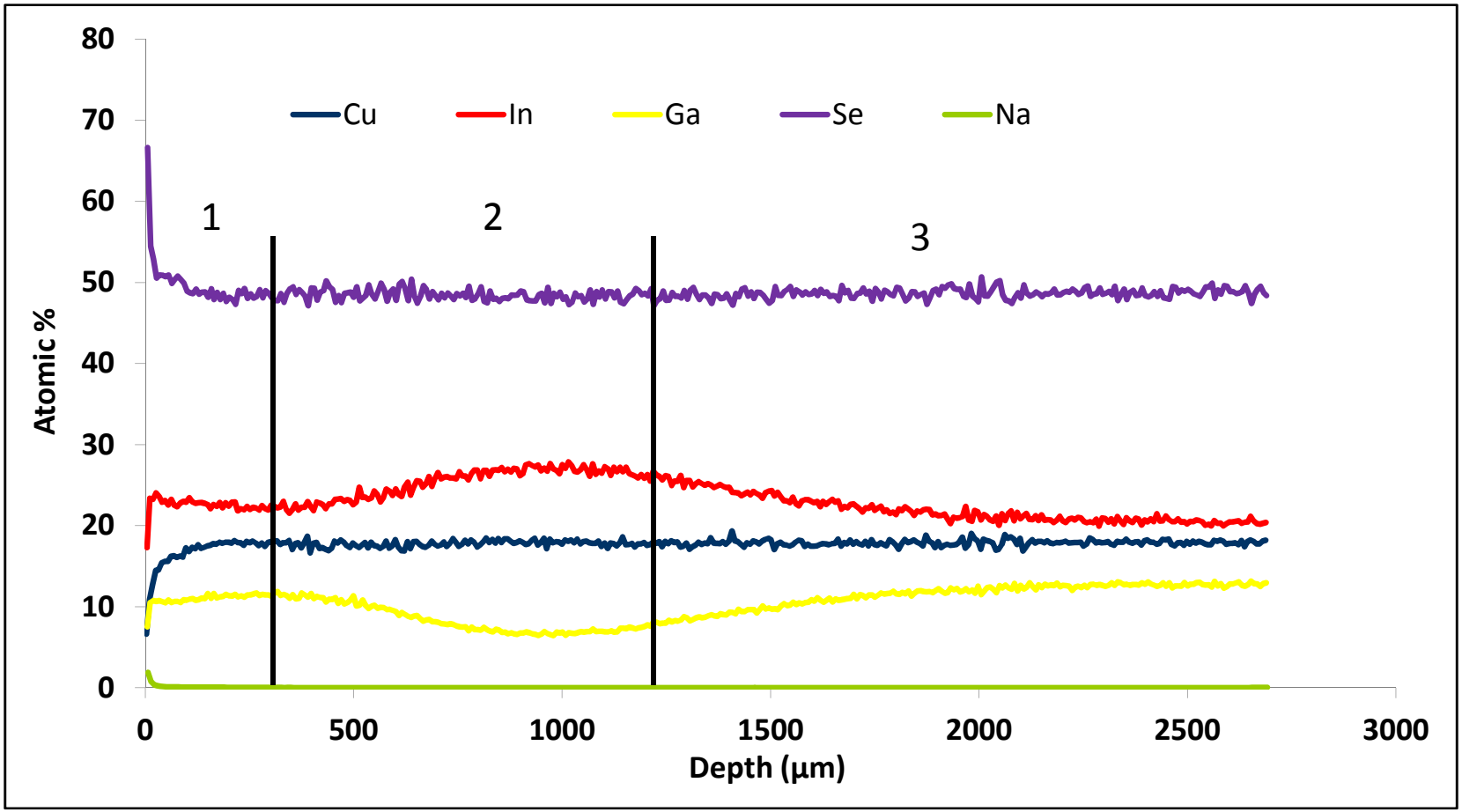
80
70
60
50
40
30
20
10
0
Atomic %
Cu
In
Ga
Se
Na
1
2
3
0
500
1000
1500
2000
2500
3000
Depth (µm)

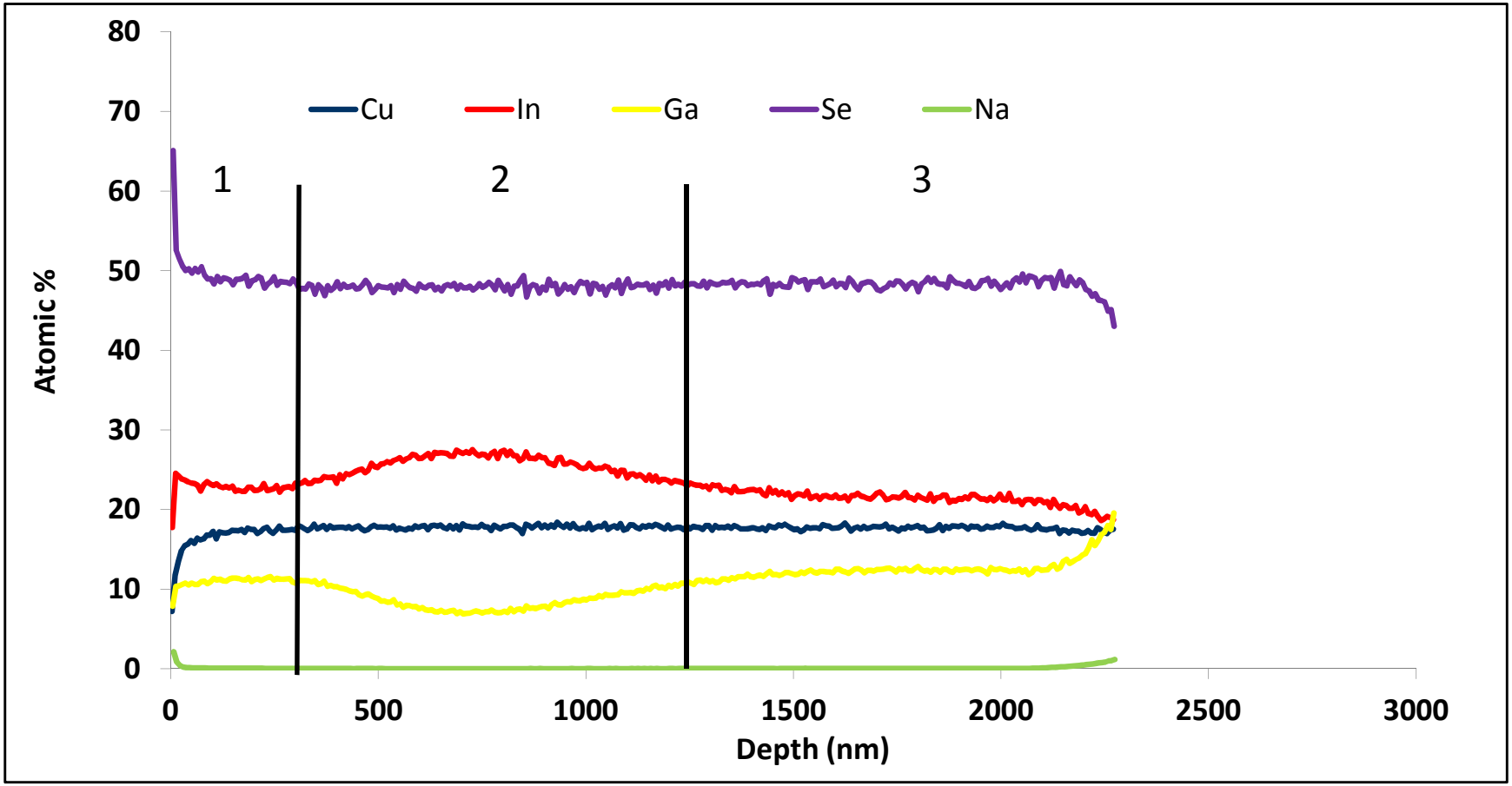
80
70
60
50
40
30
20
10
0
Atomic %
Cu
In
Ga
Se
Na
1
2
3
0
500
1000
1500
2000
2500
3000
Depth (nm)

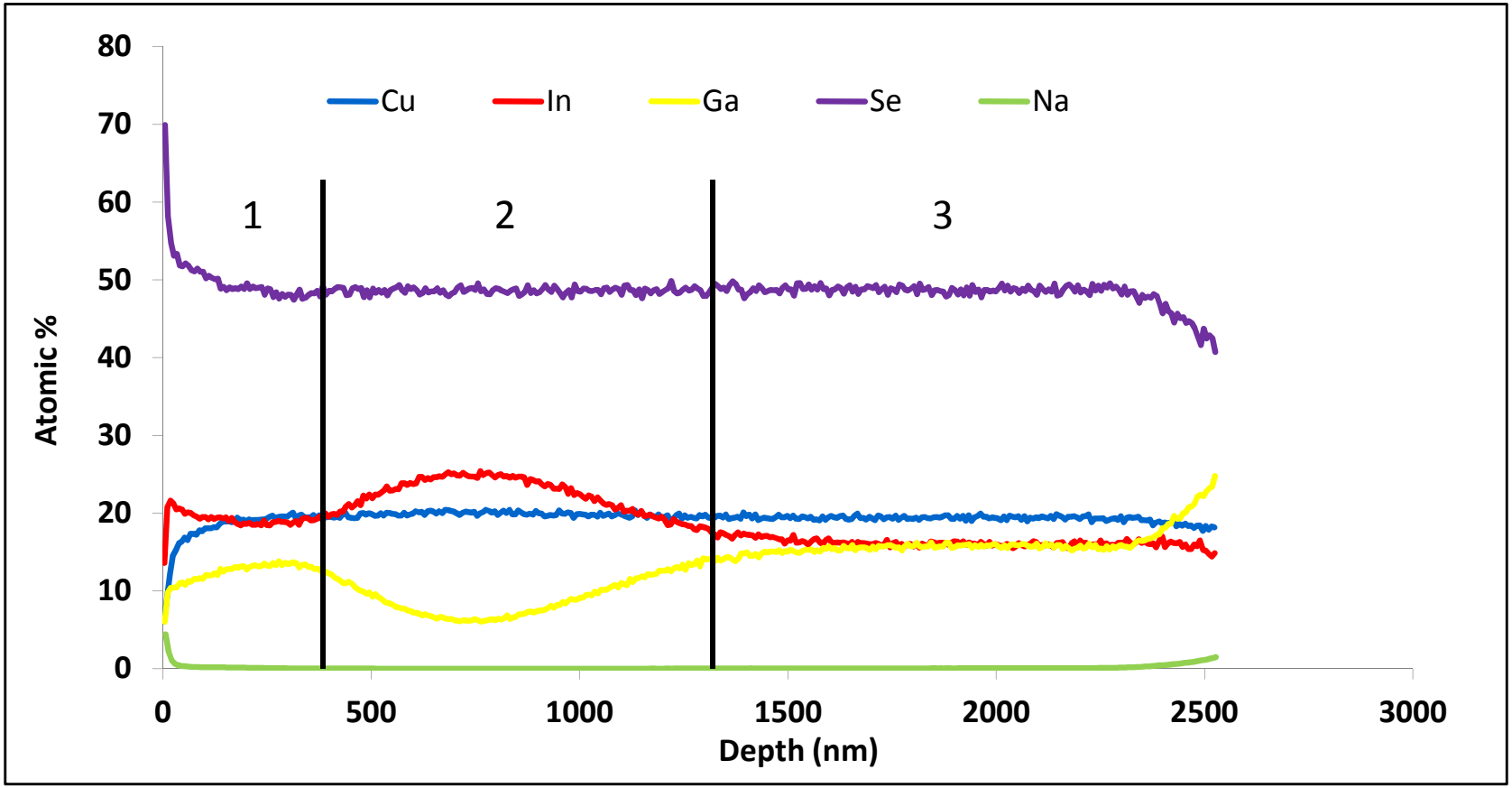
80
70
60
50
40
30
20
10
0
Atomic %
Cu
In
Ga
Se
Na
1
2
3
0
500
1000
1500
2000
2500
3000
Depth (nm)

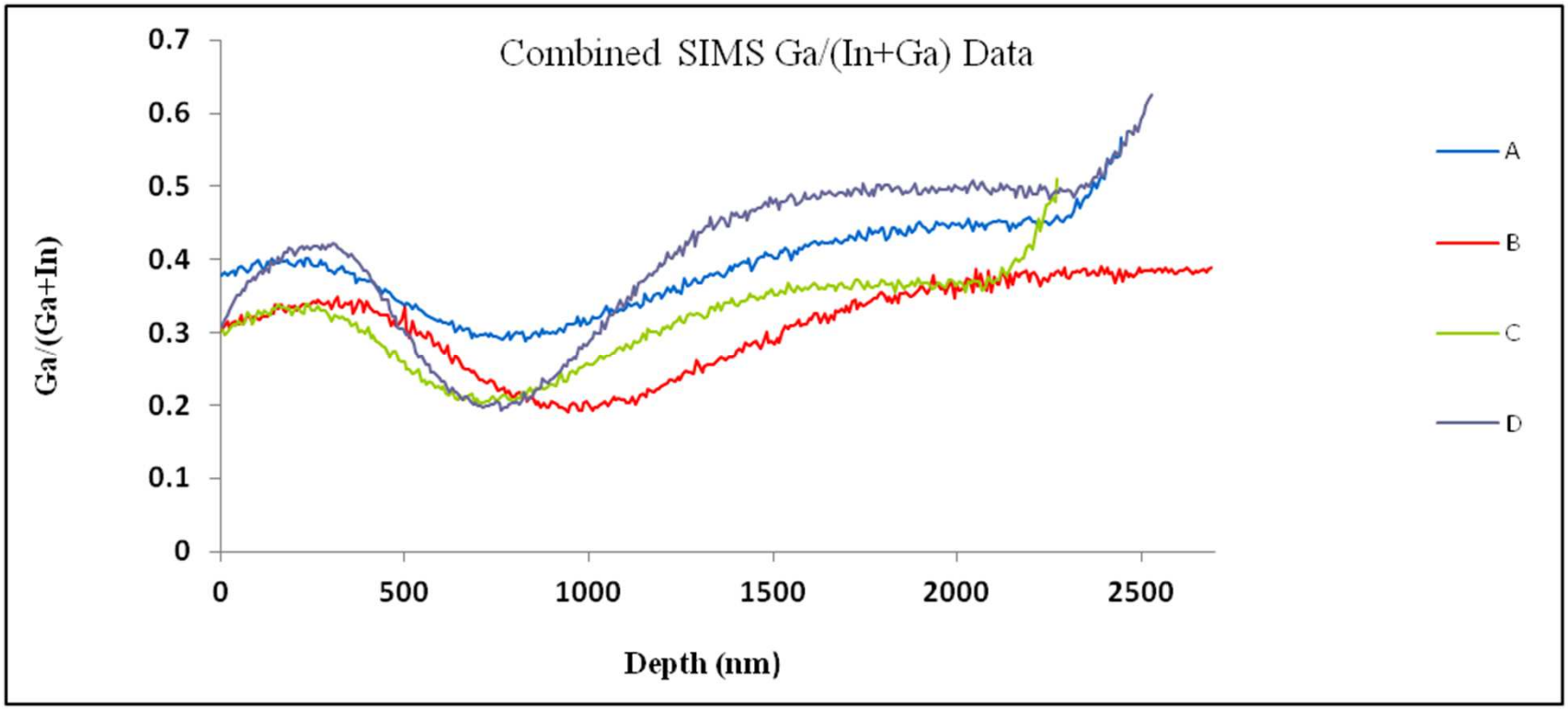
Combined SIMS Ga/(In+Ga) Data
Ga/(Ga+In)
0.7
0.6
0.5
0.4
0.3
0.2
0.1
0
0
500
1000
1500
2000
2500
Depth (nm)
A
B
C
D

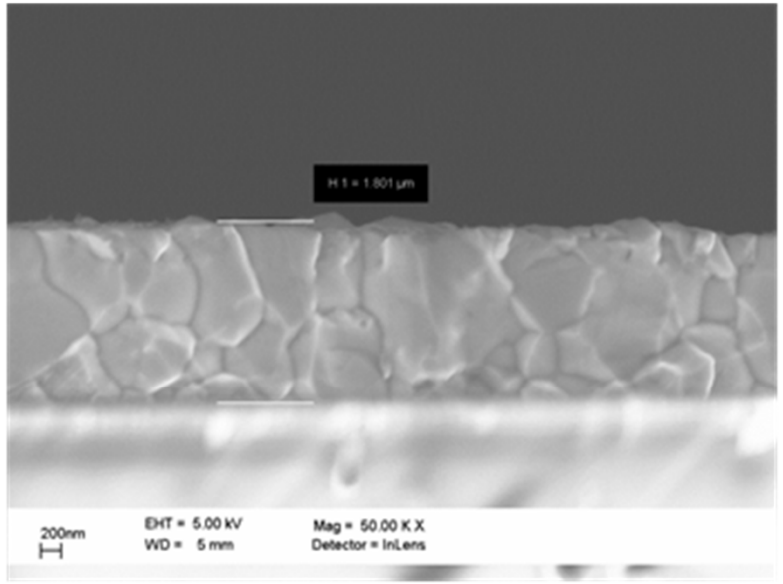
H 1 = 1.801 µm
200nm
EHT = 5.00 kV
WD = 5 mm
Mag = 50.00 K X
Detector = InLens

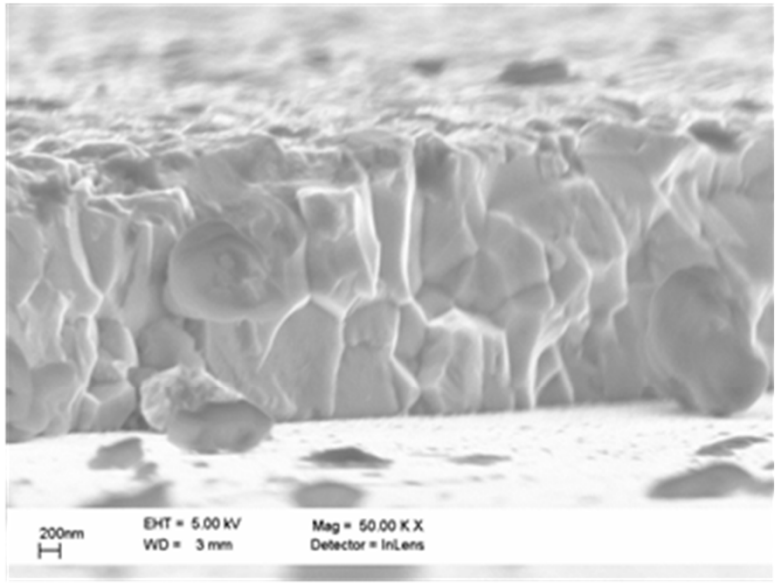
200nm
EHT = 5.00 kV
WD = 3 mm
Mag = 50.00 K X
Detector = InLens

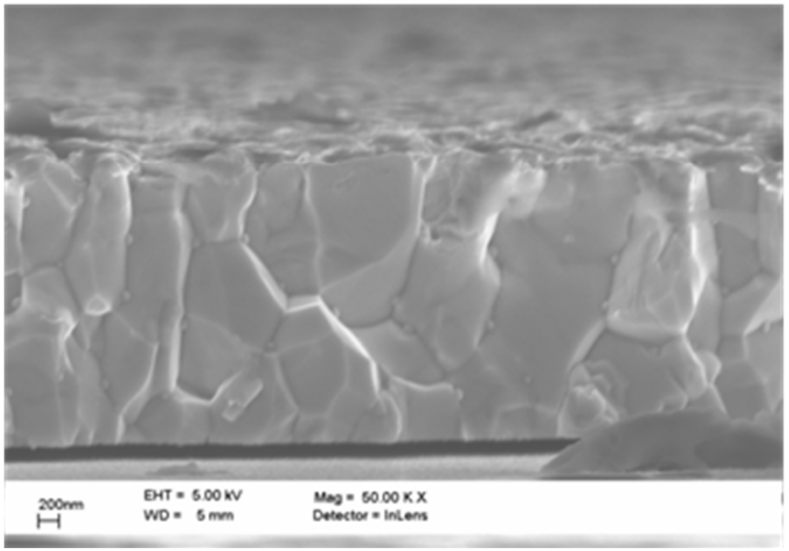
200nm
EHT = 5.00 kV
WD = 5 mm
Mag = 50.00 K X
Detector = InLens

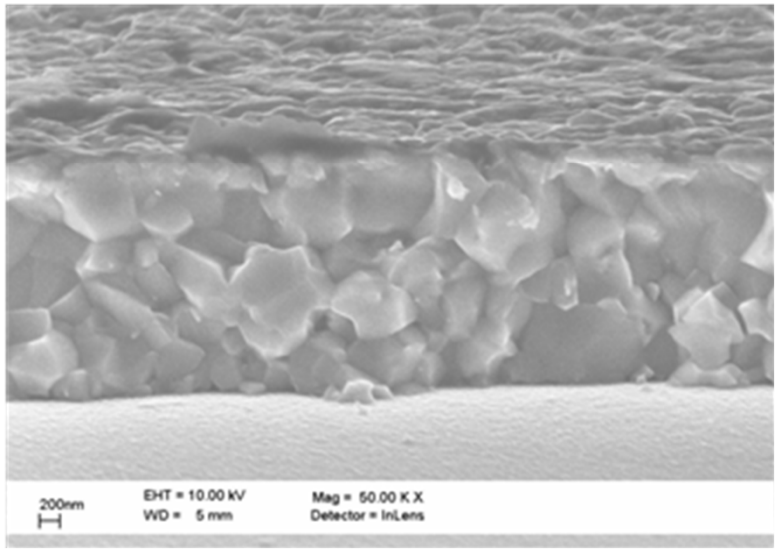
200nm
EHT = 10.00 kV
WD = 5 mm
Mag = 50.00 K X
Detector = InLens

ACCEPTED MANUSCRIPT

Highlights:

1. $Cu(In,Ga)Se_2$ (CIGS) photovoltaic (PV) films with varying Ga/(In+Ga) ratios
2. CIGS Ga ratios varying grain size
3. CIGS Ga ratio surface roughness
4. CIGS graded Ga concentration
5. Ellipsometry Tauc-Lorentz model of CIGS

ACCEPTED MANUSCRIPT